Allosteric Effects in Polynuclear Triple-Stranded Ferric Complexes

Sylvie Blanc,[†] Pnina Yakirevitch,[‡] Emmanuelle Leize,[§] Michel Meyer,[⊥] Jacqueline Libman,[‡,||] Alain Van Dorsselaer,[§] Anne-Marie Albrecht-Gary,[†] and Abraham Shanzer*[,‡]

Contribution from the Laboratoire de Physico-Chimie Bioinorganique, CNRS URA 405, ECPM, 1 rue Blaise Pascal, 67000 Strasbourg, France, Department of Organic Chemistry, Weizmann Institute of Science, Rehovot 76100, Israël, and Laboratoire de Spectrométrie de Masse Bio-Organique, CNRS URA 31, Faculté de Chimie, 1 rue Blaise Pascal, 67000 Strasbourg, France

Received July 17, 1996. Revised Manuscript Received December 5, 1996[⊗]

Abstract: The synthesis and iron(III) coordination properties of three tripodal ligands (**L**[1], **L**[2], and **L**[3]) possessing hydroxamate coordination cavities are examined by various methods (ESMS, UV−vis, CD). The ligands rely on a trisamine as anchor, which is extended by an alternating sequence of variable spacers and hydroxamates as ion binding groups. This modular strategy of design is adopted for the compounds' preparation and enables modifications of each structural element independently. The coordination properties of these iron binding molecules and particularly the presence of allosteric effects are examined by classical spectrophotometric titrations in combination with electrospray mass spectrometric measurements (ESMS). A good match between these two methods is observed, as both indicate the formation of three species in thermodynamic equilibrium: mononuclear, binuclear, and trinuclear ferric complexes. The respective stability constants are determined at p[H] = 6.5 ± 0.1 in methanol, and the corresponding distribution curves clearly illustrate the variations from ligand to ligand. These findings demonstrate that subtle structural changes have a pronounced effect on these compounds' coordination properties. Moreover, among the binders studied representatives of opposite cooperative behavior is identified. The observed dependence of the ligands' coordination properties on their structural features are rationalized.

Introduction

Allostery and cooperativity are interrelated phenomena that play a major role in biological systems.[1−3] They regulate the activity of enzymes and the recognition properties of receptors,[4] and occur when occupation of a given binding site changes the complexation characteristics of the other binding site either by improving or by reducing its binding efficiency.[5] It occurred to us that triple-stranded ligands could serve as ideal models for the study of allosteric properties in helicoidal complexes since they may be designed to possess distinct coordination sites at predetermined positions.

A large variety of helicates have been described that differ in their topology, the number of their ligands and of their guest ions, and the nature of the metals and their properties. When homopolynuclear helicates are classified according to the number of ligands that are wrapped around the metal centers, the first example consists of a single-stranded helicoidal complex that possesses two ruthenium(II) ions.[6,7] Double-stranded helicates are much more abundant. Rüttimann et al.[8] reported a dinuclear helicoidal complex with copper(I) and benzimidazole−pyridine. Lehn and co-workers synthesized double-stranded (oligobipyridine)silver(I)[9] and -copper(I)[10] helicates including up to five copper(I) ions.[11−13] Dietrich-Buchecker and Sauvage[14] used a double helicoidal copper(I) complex with two oligophenanthroline ligands as a precursor for the synthesis of the first molecular knots. Potts et al.[15] studied the occurrence of interactions in double-stranded dicuprous helicates derived from terpyridines. A stable trinuclear double helicoidal copper(II) complex of quinquepyridine was structurally characterized.[16] Constable et al.[17−20] used the oligobipyridine motif to form homobinuclear helicoidal complexes with second- and third-

* To whom correspondence should be addressed.
[†] CNRS URA 405.
[‡] Weizmann Institute of Science.
[§] CNRS URA 31.
[⊥] Present address: Department of Chemistry, University of California, Berkeley.
[||] Deceased March 1997.
[⊗] Abstract published in *Advance ACS Abstracts,* April 15, 1997.

(1) Lehn, J. M. *Supramolecular Chemistry: Concepts and Perspectives*; VCH: Weinheim, 1995.
(2) Koshland, D. E.; Neet, K. E. *Annu. Rev. Biochem.* **1968**, *37*, 359−410.
(3) Hammes, G. G.; Wu, C. W. *Annu. Rev. Biophys. Bioeng.* **1974**, *3*, 1−33.
(4) Monod, J.; Changeux, J. P.; Jacob, F. *J. Mol. Biol.* **1963**, *6*, 306−329.
(5) Perlmutter-Hayman, B. *Acc. Chem. Res.* **1986**, *19*, 90−96.
(6) Thummel, R. P.; Herry, C.; Williamson, D.; Lefoulon, F. *J. Am. Chem. Soc.* **1988**, *110*, 7894−7896.
(7) Cathey, L. J.; Constable, E. C.; Hannon, M. J.; Tocher, D. A.; Ward, M. D. *J. Chem. Soc., Chem. Commun.* **1990**, 621−622.
(8) Rüttiman, S.; Piguet, C.; Bernardinelli, G.; Bocquet, B.; Williams, A. F. *J. Am. Chem. Soc.* **1992**, *114*, 4230−4237.
(9) Garrett, T. M.; Koert, U.; Lehn, J. M. *J. Phys. Org. Chem.* **1992**, *5*, 529−532.
(10) Pfeil, A.; Lehn, J. M. *J. Chem. Soc., Chem. Commun.* **1992**, 838−839.
(11) Lehn, J. M.; Rigault, A.; Siegel, J.; Harrowfield, J.; Chevrier, B.; Moras, D. *Proc. Natl. Acad. Sci. U.S.A.* **1987**, *84*, 2565−2569.
(12) Zarges, W.; Hall, J.; Lehn, J. M.; Bolm, C. *Helv. Chim. Acta* **1991**, *74*, 1843−1851.
(13) Schoentjes, B.; Lehn, J. M. *Helv. Chim. Acta* **1995**, *78*, 1−12.
(14) Dietrich-Buchecker, C. O.; Sauvage, J. P. *Angew. Chem., Int. Ed. Engl.* **1989**, *28*, 189−192.
(15) Potts, K. T.; Keshavarz-K, M.; Tham, F. S.; Abruña, H. D.; Arana, C. R. *Inorg. Chem.* **1993**, *32*, 4450−4456.
(16) Baker, A. T.; Graig, D. C.; Dong, G. *Inorg. Chem.* **1996**, *35*, 1091−1092.
(17) Constable, E. C.; Ward, M. D. *J. Am. Chem. Soc.* **1990**, *112*, 1256−1258.
(18) Constable, E. C.; Ward, M. D.; Tocher, D. A. *J. Chem. Soc., Dalton Trans.* **1991**, 1675−1683.

S0002-7863(96)02472-9 CCC: $14.00

row transition metal elements (Cu(II), Fe(II), Pd(II), Ru(II), Cd(II), Ni(II), Mn(II)). Recently, a synthetic analog of a biscatecholate siderophore produced by the nitrogen-fixing bacterium *Azotobacter vinelandii* was shown to form a double helical dioxomolybdenum(VI) complex.[21] The diferric complex formed at neutral pH with rhodotorulic acid, a ketopiperazine bridged dihydroxamic siderophore, was the first characterized triple helicate.[22,23] The propeller-like arrangement of bidentate chelating subunits in an octahedral environment has inspired the design of various self-assembling systems forming triple helicates. Several rhodotorulic acid mimics have been synthesized by using 1,2-hydroxypyridinone,[24] catechol,[25,26] or terephthalamide[27] binding groups which favor hard metal cations like iron(III) or gallium(III). Examples of multifunctional strands incorporating soft donor atoms have also been reported.[28−33] This approach has been extended to ions of higher coordination numbers (i.e., 9) and tridentate chelating subunits by Piguet et al.,[34−37] who synthesized a rich variety of trihelicates with the aim to develop stable luminescent lanthanide complexes that could serve as light converters.

The helicoidal systems described above illustrate the rich variety of these structures and their possible applications for the generation of functional, supramolecular assemblies, mostly generated from single-stranded, symmetric ligands. However, attachment of ligands to a tripodal anchor opens the possibility to predetermine the coordinating binding cavities and to drastically reduce the number of possible complexed species, particularly when using nonsymmetric ligands. This approach is synthetically more demanding, because it necessitates covalent linkage of the ligating chains to a common anchor. Yet, the use of tripodal, asymmetric ligands enables full physicochemical characterization of these ligands' coordination properties, particularly the unambiguous characterization of each of the ligands' ion binding cavity, the preparation of site-directed, heteronuclear complexes, and the generation of assemblies with anisotropic properties. Motivated by these considerations, we initiated a program aimed at the synthesis of chiral, triple-stranded metal complexes and prepared the first homonuclear representative back in 1987,[38] and the related heteronuclear derivatives thereafter.[39]

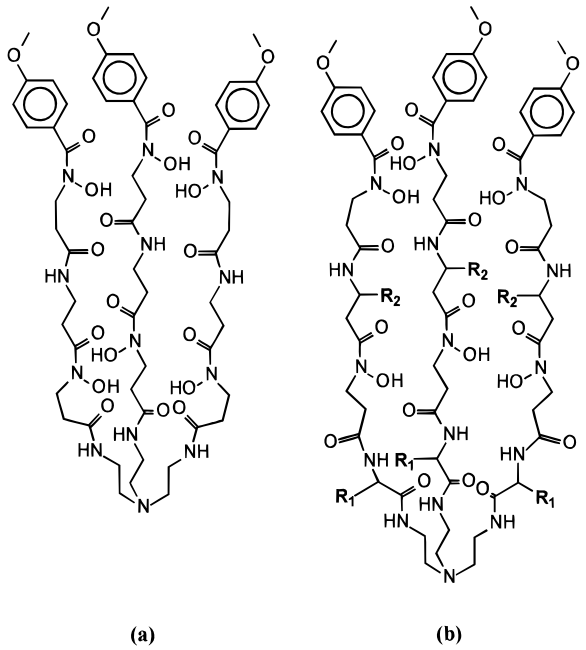

Figure 1. Chemical formulas of the tripodal hydroxamate ligands: (a) $\mathbf{L^1}$, $m = 0$, $R_2 = H$; (b) $\mathbf{L^2}$, $m = 1$, $R_1 = i$-Bu, $R_2 = H$; $\mathbf{L^3}$, $m = 1$, $R_1 = i$-Bu, $R_2 = CONEt_2$.

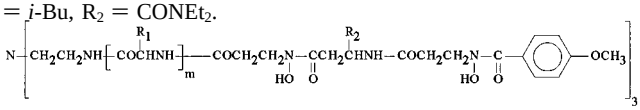

We describe here the synthesis, structural characteristics, and coordination properties of a family of three triple-stranded, polytopic ligands (Figure 1). These binders all possess hydroxamate binding cavities and bridges of the same length between the coordination sites (Figure 1), yet they differ in the spacers between the anchor and the closer hydroxamate group ($m = 0$ in $\mathbf{L^1}$, $m = 1$ in $\mathbf{L^2}$ and $\mathbf{L^3}$) and in the substituents attached to the spacers between the two hydroxamate functions ($R_2 = H$ in $\mathbf{L^1}$ and $\mathbf{L^2}$, $R_2 = CONEt_2$ in $\mathbf{L^3}$). The consequences of these subtle structural changes on the binders' coordination properties and particularly the presence of allosteric effects are examined, by applying classical spectrophotometric titrations in combination with electrospray mass spectrometric measurements (ESMS).[40−55] The combination of these two complementary methods enabled us to resolve the iron binding

(19) Constable, E. C.; Chotalia, R. *J. Chem. Soc., Chem. Commun.* **1992**, 64−66.
(20) Constable, E. C.; Hannon, M. J.; Tocher, D. A. *Angew. Chem., Int. Ed. Engl.* **1992**, *31*, 230−232.
(21) Duhme, A.-K.; Dauter, Z.; Hider, R. C.; Pohl, S. *Inorg. Chem.* **1996**, *35*, 3059−3061.
(22) Carrano, C. J.; Raymond, K. N. *J. Am. Chem. Soc.* **1978**, *100*, 5371−5374.
(23) Carrano, C. J.; Cooper, S. R.; Raymond, K. N. *J. Am. Chem. Soc.* **1979**, *101*, 599−604.
(24) Scarrow, R. C.; White, D. L.; Raymond, K. N. *J. Am. Chem. Soc.* **1985**, *107*, 6540−6546.
(25) Enemark, E. J.; Stack, T. D. P. *Angew. Chem., Int. Ed. Engl.* **1995**, *34*, 996−998.
(26) Enemark, E. J.; Stack, T. D. P *Inorg. Chem.* **1996**, *35*, 2719−2720.
(27) Kersting, B.; Meyer, M.; Powers, R. E.; Raymond, K. N. *J. Am. Chem. Soc.* **1996**, *30*, 7221−7222.
(28) Krämer, R.; Lehn, J. M.; De Cian, A.; Fischer, J. *Angew. Chem., Int. Ed. Engl.* **1993**, *32*, 703−706.
(29) Krämer, R.; Lehn, J. M.; Marquis-Rigault, A. *Proc. Natl. Acad. Sci. U.S.A.* **1993**, *90*, 5394−5398.
(30) Williams, A. F.; Piguet, C.; Bernardinelli, G. *Angew. Chem., Int. Ed. Engl.* **1991**, *30*, 1490−1492.
(31) Charbonniere, L.; Bernardinelli, G.; Piguet, C.; Sargeson, A. M.; Williams, A. F. *J. Chem. Soc., Chem. Commun.* **1994**, 1419−1420.
(32) Piguet, C.; Bernardinelli, G.; Bocquet, B.; Schaad, O.; Williams, A. F. *Inorg. Chem.* **1994**, *33*, 4112−4121.
(33) Zurita, D.; Baret, P.; Pierre, J. L. *New J. Chem.* **1994**, *18*, 1143−1146.
(34) Bernardinelli, G.; Piguet, C.; Williams, A. F. *Angew. Chem., Int. Ed. Engl.* **1992**, *31*, 1622−1624.
(35) Piguet, C.; Williams, A. F.; Bernardinelli, G.; Bünzli, J. C. *Inorg. Chem.* **1993**, *32*, 4139−4149.
(36) Piguet, C.; Bünzli, J. C.; Bernardinelli, G.; Hopfgartner, G.; Williams, A. F. *J. Am. Chem. Soc.* **1993**, *115*, 8197−8206.
(37) Piguet, C.; Bünzli, J. C.; Bernardinelli, G.; Bochet, C. F.; Froidevaux, P. *J. Chem. Soc., Dalton Trans.* **1995**, 83−97.
(38) Libman, J.; Tor, Y.; Shanzer, A. *J. Am. Chem. Soc.* **1987**, *109*, 5880−5881.
(39) Zelikovich, L.; Libman, J.; Shanzer, A. *Nature* **1995**, *374*, 790−792.
(40) Bruins, A. P.; Covey, T. R.; Henion, J. D. *Anal. Chem.* **1987**, *59*, 2642−2646.
(41) Fenn, J. B.; Mann, M.; Meng, C. K.; Wong, S. F.; Whitehouse, C. M. *Mass Spectrom. Rev.* **1990**, *9*, 37−70.
(42) Bruins, A. P. *Mass Spectrom. Rev.* **1991**, *10*, 53−77.
(43) Bitsch, F.; Dietrich-Buchecker, C.; Khemiss, A. K.; Sauvage, J. P.; Van Dorsselaer, A. *J. Am. Chem. Soc.* **1991**, *113*, 4023−4025.
(44) Katta, V.; Chowdhury, S. K.; Chait, B. T. *J. Am. Chem. Soc.* **1990**, *112*, 5348−5349.
(45) Ashton, P. R.; Brown, C. L.; Chapman, J. R.; Gallagher, R. T.; Stoddardt, J. F. *Tetrahedron Lett.* **1992**, *33*, 7771−7774.
(46) Przybylski, M.; Glocker, M. O. *Angew. Chem., Int. Ed. Engl.* **1996**, *35*, 806−826.
(47) Jaquinod, M.; Leize, E.; Potier, N.; Albrecht, A. M.; Shanzer, A.; Van Dorsselaer, A. *Tetrahedron Lett.* **1993**, *34*, 2771−2774.
(48) Leize, E.; Van Dorsselaer, A.; Krämer, R.; Lehn, J. M. *J. Chem. Soc., Chem. Commun.* **1993**, 990−993.
(49) Russell, K. C.; Leize, E.; Van Dorsselaer, A.; Lehn, J. M. *Angew. Chem., Int. Ed. Engl.* **1995**, *34*, 209−213.

Scheme 1

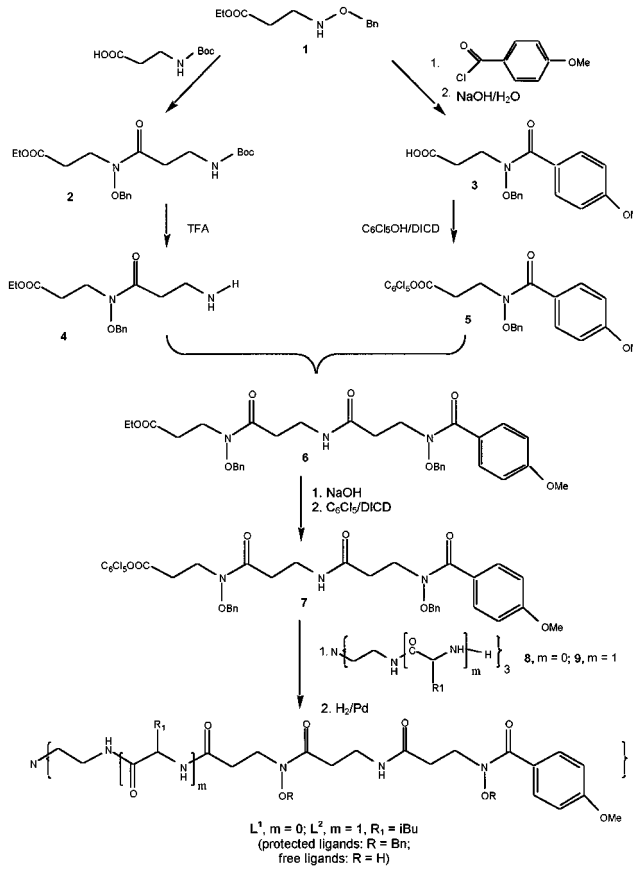

Scheme 2

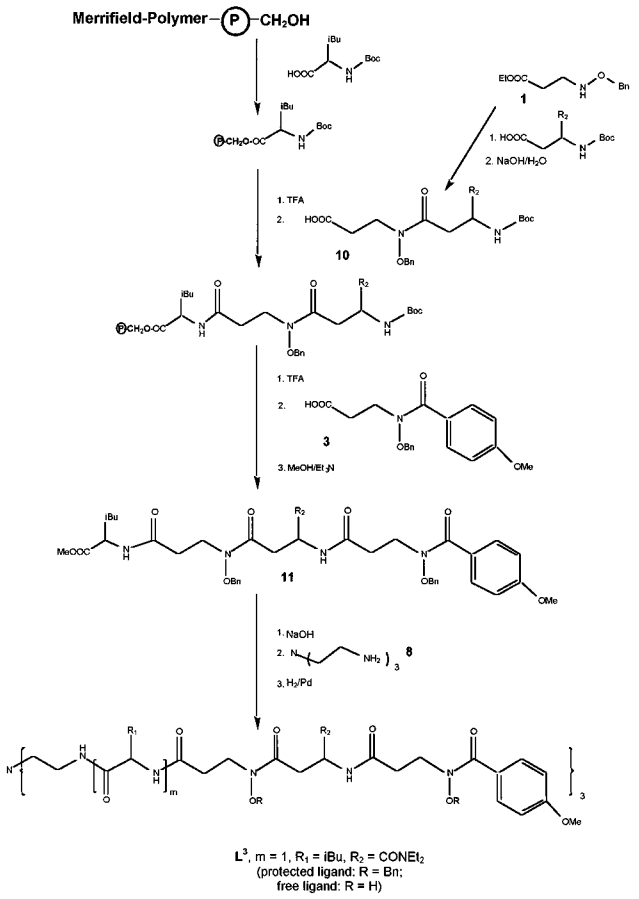

properties of the ligands considered in this work, to determine the nature of their ferric species, to measure their respective stability constants and absorption spectra, to ascertain the distribution of the different species at any given ligand/iron ratios, and to quantify the interactions between the two trihydroxamate ion binding cavities.

Results

Synthesis. A modular strategy was adopted for the ligands' synthesis, as outlined in Schemes 1 and 2. According to this strategy the triple-stranded binders were synthesized from three elements: an anchor, a hydroxamate-containing, variable intermittent monomer, and a hydroxamate group containing a terminal monomer. As anchor we used the achiral tris(2-aminoethyl)amine (**8**), which was optionally extended by a leucyl residue as spacer to **9**. As ion binding monomer we employed either the achiral hydroxamate **2** assembled from 3-(*N*-hydroxyamino)propionic acid and β-alanine or its chiral congener **10** derived from 3-(*N*-hydroxyamino)propionic acid and aspartic acid. As terminal group we selected the benzoylated 3-(*N*-hydroxyamino)propionic acid **3**.

The triple-stranded binders were accordingly synthesized in either of two sequences. In the first sequence (Scheme 1) the intermittent **2** and terminal **3** monomers were linked together to the dihydroxamate **6**, and subsequently coupled to the anchor **8** and its extended congener **9**. Ligands $\mathbf{L^1}$ and $\mathbf{L^2}$ were prepared according to this sequence. In the second sequence (Scheme 2) the ligating chains were assembled by the Merrifield method of synthesis before condensation to the trisamine **8**. According to this sequence, leucine, intermittent monomer **10**, and terminal monomer **3** were successively linked to the Merrifield resin, applying coupling methods commonly used in peptide synthesis. The immobilized chain was then removed from the solid support, purified, and condensed to the anchor to provide ligand $\mathbf{L^3}$ after hydrogenation.

All intermediates and final products were fully characterized by their IR and ^{1}H NMR spectra, also partly by COESY spectra, as described in the Experimental Section, and by their MS spectra which are summarized in Table 1.

Electrospray Mass Spectra. As an example, the electrospray mass spectra recorded for ligand $\mathbf{L^1}$ at four different $[\mathbf{L^1}]_{tot}/[Fe(III)]_{tot}$ ratios are presented in Figure 2. The mass spectrometric study clearly showed the formation of three ferric complexes in thermodynamic equilibrium. The pseudomolecular ions of the different species observed with **L** (**L** = $\mathbf{L^1}$, $\mathbf{L^2}$, and $\mathbf{L^3}$) in the ES mass spectra are given in Table 1.

For **L**, **L**Fe, and **L**Fe$_2$, only doubly-charged ions were obtained. The major ionization was obtained by the diprotonation of the ligand. The minor peaks at -16 Da in the free ligands and in the three corresponding ferric complexes could be related to a minor reduction process of a single hydroxamate function which has been widely observed by FAB mass spectrometry in siderophores, but not fully elucidated.[56−58] One

(50) Marquis-Rigault, A.; Dupont-Gervais, A.; Baxter, P. N. W.; Van Dorsselaer, A.; Lehn, J. M. *Inorg. Chem.* **1996**, *35*, 2307−2310.
(51) Hopfgartner, G.; Piguet, C.; Henion, J. D.; Williams, A. F. *Helv. Chim. Acta* **1993**, *76*, 1759−1766.
(52) Hopfgartner, G.; Piguet, C.; Henion, J. D. *J. Am. Soc. Mass Spectrom.* **1994**, *5*, 748−756.
(53) Caudle, M. T.; Stevens, R. D.; Crumbliss, A. L. *Inorg. Chem.* **1994**, *33*, 843−844.
(54) Caudle, M. T.; Stevens, R. D.; Crumbliss, A. L. *Inorg. Chem.* **1994**, *33*, 6111−6115.
(55) Cheng, X.; Gao, Q.; Smith, R. D.; Simanek, E. E.; Mammen, M.; Whitesides, G. M. *J. Org. Chem.* **1996**, *61*, 2204−2206.
(56) Dell, A.; Hider, R. C.; Barber, M.; Bordoli, R. S.; Sedgwick, Tyler, A. N.; Neilands, J. B. *Biomed. Mass Spectrom.* **1982**, *9*, 158−161

Table 1. ESMS Data Ferric $\mathbf{L^1}$, $\mathbf{L^2}$, and $\mathbf{L^3}$ Complex Pseudomolecular Ions in Methanol

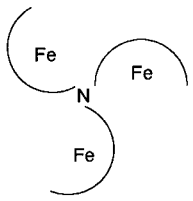

		m/z		*m/z*		*m/z*		*m/z*
	$[L - 16 + 2H]^{2+}$	635.0	$[LFe - 16 + 2H]^{2+}$	661.4	$[LFe_2 - 16 + 2H]^{2+}$	688.1	$[LFe_3]^{3+}$	482.1
	$[L + 2H]^{2+}$	643.1	$[LFe + 2H]^{2+}$	669.7	$[LFe_2 + 2H]^{2+}$	696.1	$[LFe_3 + Cl + K]^{3+}$	506.5
$\mathbf{L^1}$	$[L + H + Na]^{2+}$	654.1	$[LFe + H + Na]^{2+}$	680.8	$[LFe_2 + H + Na]^{2+}$	707.1	$[LFe_3 - H]^{2+}$	722.3
	$[L + H + K]^{2+}$	662.2	$[LFe + H + K]^{2+}$	688.8	$[LFe_2 + H + K]^{2+}$	715.0	$[LFe_3 - 16 + Cl]^{2+}$	732.3
							$[LFe_3 - H + MeOH]^{2+}$	738.5
							$[LFe_3 + Cl]^{2+}$	740.4
	$[L - 16 + 2H]^{2+}$	803.9	$[LFe - 16 + 2H]^{2+}$	831.3	$[LFe_2 - 16 + 2H]^{2+}$	857.7	$[LFe_3 - 16 - H]^{2+}$	884.2
$\mathbf{L^2}$	$[L + 2H]^{2+}$	811.5	$[LFe + 2H]^{2+}$	839.2	$[LFe_2 + 2H]^{2+}$	865.7	$[LFe_3 - H]^{2+}$	892.3
	$[L + H + Na]^{2+}$	822.3	$[LFe + H + Na]^{2+}$	850.5	$[LFe_2 + H + Na]^{2+}$	876.7	$[LFe_3 - 16 - H + MeOH]^{2+}$	901.0
			$[LFe + H + K]^{2+}$	858.3	$[LFe_2 + H + K]^{2+}$	884.7	$[LFe_3 - H + MeOH]^{2+}$	908.2
	$[L - 16 + 2H]^{2+}$	953.6	$[LFe - 16 + 2H]^{2+}$	979.9	$[LFe_2 - 16 + 2H]^{2+}$	1006.4	$[LFe_3 - H]^{2+}$	1041.5
$\mathbf{L^3}$	$[L + 2H]^{2+}$	961.5	$[LFe + 2H]^{2+}$	988.1	$[LFe_2 + 2H]^{2+}$	1014.5	$[LFe_3 - 16 - H + MeOH]^{2+}$	1049.5
	$[L + H + Na]^{2+}$	972.5	$[LFe + H + Na]^{2+}$	999.0	$[LFe_2 + H + Na]^{2+}$	1025.5	$[LFe_3 - H + MeOH]^{2+}$	1057.0
	$[L + H + K]^{2+}$	980.6	$[LFe + H + K]^{2+}$	1006.9				

could also notice the cationization with Na^+ and K^+ of the different species, **L**, **L**Fe, and **L**Fe_2. The mass difference measured between these three species was about 52.7 Da, demonstrating that the complexation by each of the ferric ions was accompanied by loss of three protons from the hydroxamate groups. On the other hand, the complexation of the third ferric ion was not accompanied by loss of three protons, but by the appearance of three positive charges, in agreement with the **L**Fe_3, $3Cl^-$ species. In this case, the major ionization did not occur by protonation of the ligand **L**, but by loss of two or three Cl^- counterions. The complex **L**Fe_3 was thus characterized by distinct pseudomolecular ions of different charge states such as $[\mathbf{L}Fe_3]^{3+}$, $[\mathbf{L}Fe_3 - H]^{2+}$, and $[\mathbf{L}Fe_3 + Cl]^{2+}$. In the case of **L**$Fe_3$, cationization with K^+ and an addition of methanol were also observed. The peaks indicated by an asterisk in the mass spectra were shown to derive from the $FeCl_3$ solution.

Stability Constants. The global stability constants of the ferric complexes formed with the polytopic binders $\mathbf{L^1}$, $\mathbf{L^2}$, and $\mathbf{L^3}$ were determined by spectrophotometric titrations of the free ligand with iron(III). As an example, a batch titration of receptor $\mathbf{L^1}$ is shown in Figure 3 up to a 3.5-fold excess of iron(III).

For each ligand, the best fit of the spectrophotometric data was obtained with the model including three ferric species, a mono-, a di-, and a trinuclear complex, in agreement with the mass spectrometric observations. The values of the global stability constants obtained for the three **L**Fe, **L**Fe_2, and **L**Fe_3 complexes with the three ligands $\mathbf{L}^1$, $\mathbf{L}^2$, and $\mathbf{L}^3$ respectively, are summarized in Table 2.

For ligand $\mathbf{L^1}$ the stability constants of the mono- and diferric complexes were also determined by competition experiments using CDTA as scavenger (Figure 4). The stability constant of the trinuclear complex could not be determined from these experiments, since the ferric $\mathbf{L^1}$ solution used for titration with CDTA contained 2 equiv of iron(III)/equiv of ligand. The preliminary independent determination of the apparent stability constant of CDTAFe(III) at $p[H] = 6.5 \pm 0.1$ in methanol gave a log K_{CDTAFe} value of 6.8 ± 0.3 at 25.0 ± 0.1 °C and $I = 0.05$ M. Two different statistical methods (relying on the Letagrop-Spefo[62,63] and Specfit[59−61] programs) were used to determine the stability constants presented in Table 2. The most precise data were obtained with the Letagrop program.[62,63] The lack of a pit-mapping adjustment in the recent Specfit software[59−61] led to larger uncertainties. Yet, the key values obtained by either method were in very good agreement (Table 2). For further calculations, only the data fitted with the Letagrop program[62,63] were used. In the case of $\mathbf{L^1}$, for which binding constants were determined by both methods, a direct one and a competitive one, only the average value will be used in the following discussion.

Absorption UV−Vis Spectra. The electronic spectra corresponding to the $\mathbf{L}^1$, $\mathbf{L}^2$, and $\mathbf{L}^3$ mono-, di-, and triferric complexes were calculated by both the Specfit[59−61] and Letagrop-Spefo[62,63] programs. The respective spectra are presented in Figure 5. A typical charge-transfer band for trihydroxamate ferric species is observed at 435 ± 10 nm for all the mono- and diferric complexes. The formation of triferric species induces a bathochromic shift of 5−25 nm, as expected for dihydroxamate binding.

(57) De Hoffmann E.; Stroobant, V. *Biol. Mass Spectrom.* **1991**, *20*, 142−152.
(58) Mohn, G.; Taraz, K.; Budzikiewicz, H. *Z. Naturforsch.* **1990**, *45b*, 1437−1450.
(59) Gampp, H.; Maeder, M; Meyer, C. J.; Zuberbühler, A. D. *Talanta* **1985**, *32*, 95−101.
(60) Gampp, H.; Maeder, M; Meyer, C. J.; Zuberbühler, A. D. *Talanta* **1986**, *33*, 943−951.
(61) Gampp, H.; Maeder, M; Meyer, C. J.; Zuberbühler, A. D. *Comments Inorg. Chem.* **1987**, *6*, 41−60.
(62) Sillen, L. G.; Warnqvist, B. *Ark. Kemi* **1968**, *31*, 377−390.
(63) Arnek, R.; Sillen, L. G.; Wahlberg, O. *Arkiv för Kemi* **1968**, *31*, 353−363.

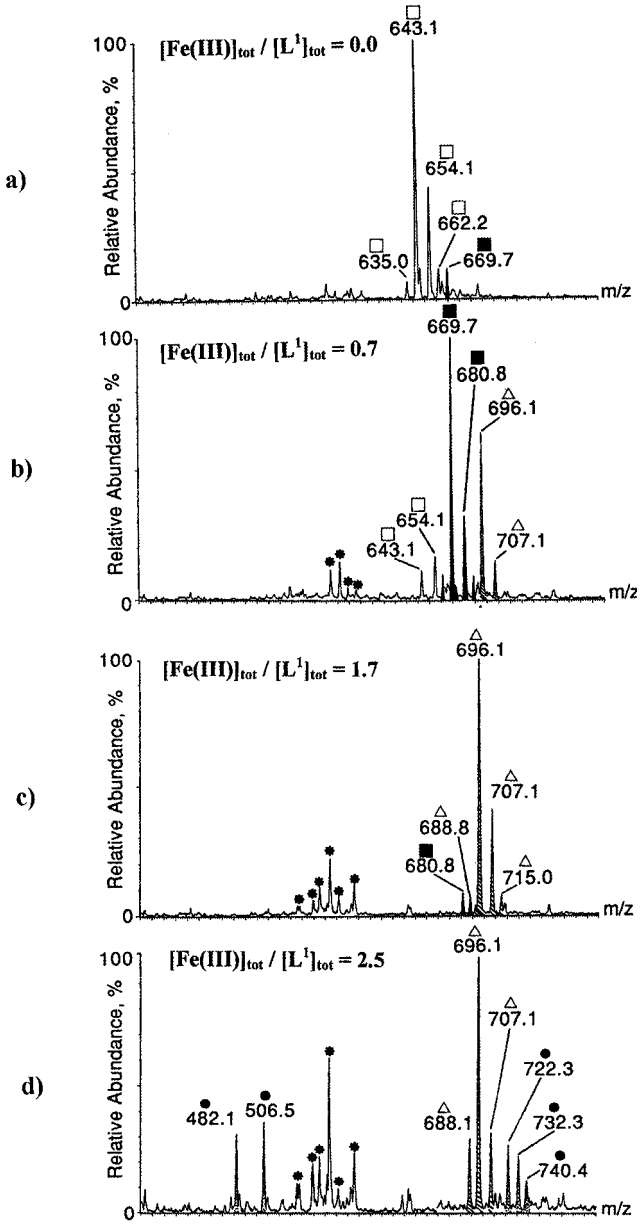

Figure 2. ES mass spectra of $\mathbf{L^1}$ ferric complexes in methanol (□, $\mathbf{L^1}$; ■, $\mathbf{L^1}Fe$; △, $\mathbf{L^1}Fe_2$; ●, $\mathbf{L^1}Fe_3$; *, impurities coming from the $FeCl_3$ solution): $[\mathbf{L^1}]_{tot} = 2.0 \times 10^{-5}$ M (a); $[\mathbf{L^1}]_{tot} = 2.0 \times 10^{-5}$ M, $[Fe(III)]_{tot} = 1.4 \times 10^{-5}$ M (b); $[\mathbf{L^1}]_{tot} = 2.0 \times 10^{-5}$ M, $[Fe(III)]_{tot} = 3.4 \times 10^{-5}$ M (c); $[\mathbf{L^1}]_{tot} = 2.0 \times 10^{-5}$ M, $[Fe(III)]_{tot} = 5.0 \times 10^{-5}$ M (d).

Discussion

In order to obtain triple-stranded, helicoidal ion binding molecules that could accommodate two metal ions in their inner space, a C_3-symmetric trisamine as anchor has been selected and extended by a sequence of two alternating, bidentate ion binding sites and amide-containing spacers. The three strands, possessing each of the two hydroxamate sites, create two binding cavities for metals of octahedral coordination geometries. The amide-containing spacers induce interstrand H-bonds such as to minimize random coiling and to stabilize specific conformations. This type of assembly enables systematic modifications by varying the nature of the ion binding sites, the length of the spacers and their projecting substituents, and chiralities. The latter possibilities were realized in this work with the synthesis of ligands $\mathbf{L}^1$, $\mathbf{L}^2$, and $\mathbf{L}^3$.

The three polytopic ligands were prepared in a modular fashion from several common elements by either of two methods, a batch method (Scheme 1) or a solid-state method (Scheme 2). For the ligands prepared the two methods proved comparable. Yet, when extension of these binders to polytopic ion binders is considered, the solid-state, Merrifield method is by far superior.[64]

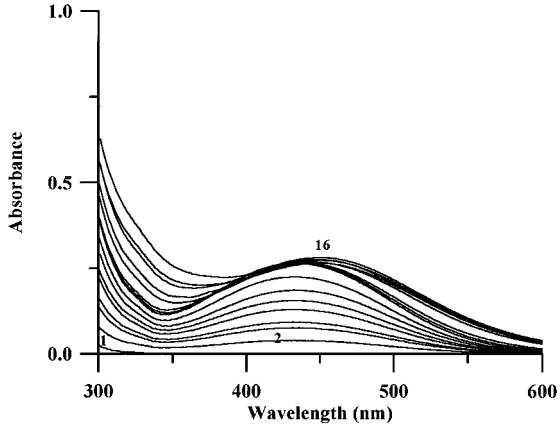

Figure 3. Spectrophotometric titration of the ligand $\mathbf{L^1}$ by iron(III): solvent methanol; p[H] = 6.5 ± 0.1; $I = 0.05$; $T = 25.0 \pm 0.1$ °C; $l = 1$ cm; $[\mathbf{L^1}]_{tot} = 4.5 \times 10^{-5}$ M; spectra 1−16, $[Fe(III)]_{tot} = 0$, 1.0×10^{-5}, 1.8×10^{-5}, 2.7×10^{-5}, 3.6×10^{-5}, 4.5×10^{-5}, 5.3×10^{-5}, 6.3×10^{-5}, 7.3×10^{-5}, 8.0×10^{-5}, 9.1×10^{-5}, 1.08×10^{-4}, 1.17×10^{-4}, 1.26×10^{-4}, 1.44×10^{-4}, 1.58×10^{-4} M, respectively.

FT-IR and ^{1}H NMR spectroscopy of the free ligands and their benzylated, protected precursors indicated the presence of extensive H-bond networks. Thus, the stretching frequencies of the amide NH groups were consistently close to 3300 cm^{-1} when measured in diluted chloroform solutions (<5 mM). The ^{1}H NMR spectra of the chiral ligands $\mathbf{L^2}$ and $\mathbf{L^3}$ revealed pronounced nonequivalence of their diastereotopic protons $-CH_2NOCO-$ and $-NCH_2CH_2-$ even in protic solvents. The combination of these phenomena, short-frequency NH absorptions, and pronounced nonequivalence of diastereotopic protons has earlier been demonstrated to result from interstrand H-bonds which restrict the compounds' conformational freedom.[65−67] The IR spectra of the ferric complexes of all ligands also showed low-frequency NH absorptions (see the Experimental Section), indicating preservation (or even strengthening) of the ligands' H-bond network.

Using both ESMS and UV−vis absorption spectrophotometry, three distinct ferric complexes were identified upon titration of the tripodal ligands $\mathbf{L^1}$, $\mathbf{L^2}$, and $\mathbf{L^3}$ in $[Fe(III)]_{tot}/[ligand]_{tot}$ ratios between 0.2 and 4.0, in methanol at p[H] = 6.5. In order to quantify the interactions between the two trihydroxamate metal centers and to evaluate the competition between the dinuclear and trinuclear complexes, we present in Table 3 the respective stability constants. The latter were calculated by fitting experimental data with the Letagrop program[62,63] (Table 2), as already discussed.

Ferrioxamine B was used as a reference for the trihydroxamate monoferric complexes. Its stability constant in methanol at p[H] = 6.3 ± 0.1, $I = 0.1$ M, and $T = 25.0 \pm 0.1$ °C was determined to be $\log K_{\text{ferrioxamine B}} = 7.17 \pm 0.03$. Comparison between the $K_{\text{ferrioxamine B}}$ value of ferrioxamine B and the K_1 values for the monoferric complexes of the ligands $\mathbf{L^1}$, $\mathbf{L^2}$, and

(64) Stewart, J. M.; Young, J. D. *Solid Phase Peptide Synthesis*, 2nd ed.; Pierce Chemical Co.: Rockford, IL, 1984; p 176.
(65) Tor, Y.; Libman, J.; Shanzer, A.; Felder, C. E.; Lifson, S. *J. Am. Chem. Soc.* **1992**, *114*, 6653−6661.
(66) Tor, Y.; Libman, J.; Shanzer, A.; Felder, C. E.; Lifson, S. *J. Am. Chem. Soc.* **1992**, *114*, 6661−6671.
(67) Dayan, I.; Libman, J.; Agi, Y.; Shanzer, A. *Inorg. Chem.* **1993**, *32*, 1467−1475.

Table 2. $\mathbf{L^1}$, $\mathbf{L^2}$, and $\mathbf{L^3}$ Ferric Complexes: Global Stability Constants[a]

equilibrium	$\log \beta \pm 3\sigma$ $\mathbf{L^1}$	$\mathbf{L^2}$	$\mathbf{L^3}$
$L + Fe(III) \overset{\beta_1}{\rightleftharpoons} LFe(III)$	5.95 ± 0.04[b] (6.1 ± 0.9)[c] 5.70 ± 0.07[b,d] (5.2 ± 1.2)[c,d]	6.60 ± 0.03[b] (6.6 ± 0.8)[c]	6.75 ± 0.04[b] (6.6 ± 0.5)[c]
$L + 2Fe(III) \overset{\beta_2}{\rightleftharpoons} LFe(III)_2$	12.21 ± 0.02[b] (12.2 ± 0.5)[c] 12.08 ± 0.04[b,d] (12.1 ± 0.6)[c,d]	12.10 ± 0.05[b] (12.1 ± 0.6)[c]	12.80 ± 0.05[b] (12.6 ± 0.4)[c]
$L + 3Fe(III) \overset{\beta_3}{\rightleftharpoons} LFe(III)_3$	16.8 ± 0.1[b] (16.8 ± 0.5)[c]	17.20 ± 0.08[b] (17.4 ± 0.8)[c]	17.6 ± 0.1[b] (17.6 ± 0.4)[c]

[a] Solvent methanol; p[H] = 6.5 ± 0.1; I = 0.05 M; T = 25.0 ± 0.1 °C. [b] Values fitted with the Letagrop program.[62,63] [c] Values fitted with the Specfit program[59−61] and not used for further calculations. [d] Calculated from the competition titration with CDTA.

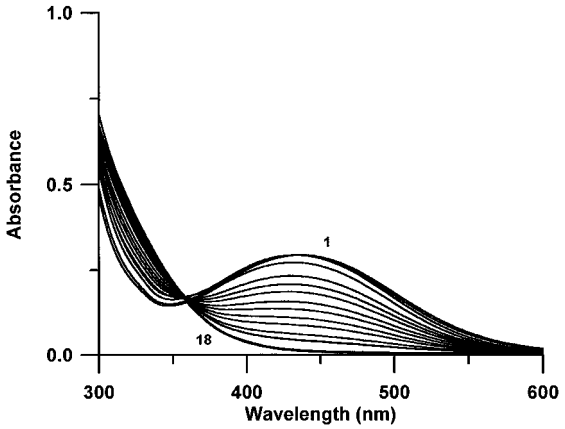

Figure 4. Spectrophotometric competition titration of $\mathbf{L^1}$ ferric complexes by CDTA: solvent methanol; p[H] = 6.5 ± 0.1; I = 0.05; T = 25.0 ± 0.1 °C; l = 1 cm; $[\mathbf{L^1}]_{tot} = 4.5 \times 10^{-5}$ M; $[Fe(III)]_{tot} = 9.0 \times 10^{-5}$; spectra 1−18; $[CDTA]_{tot}$ = 0, 0.9×10^{-5}, 1.8×10^{-5}, 2.7×10^{-5}, 3.7×10^{-5}, 4.5×10^{-5}, 5.4×10^{-5}, 6.4×10^{-5}, 7.3×10^{-5}, 8.2×10^{-5}, 9.1×10^{-5}, 1.00×10^{-4}, 1.09×10^{-4}, 1.18×10^{-4}, 1.27×10^{-4}, 1.36×10^{-4}, 1.60×10^{-4}, 1.82×10^{-4} M, respectively.

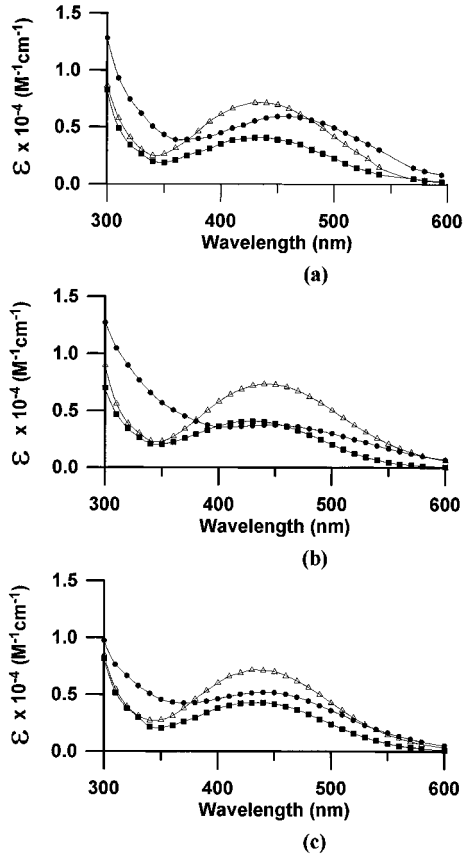

Figure 5. Calculated electronic spectra of mono- (■), di- (△), and triferric (●) complexes formed with $\mathbf{L^1}$ (a), $\mathbf{L^2}$ (b), and $\mathbf{L^3}$ (c): solvent methanol; p[H] = 6.5 ± 0.1; I = 0.05; T = 25.0 ± 0.1 °C.

$\mathbf{L^3}$ under analogous conditions reveals destabilization of the $\mathbf{L^1}$, $\mathbf{L^2}$, and $\mathbf{L^3}$ monoferric complexes of about 1 order of magnitude (Table 3). This result could be explained by a more strained tripodal structure compared with the flexible linear structure of desferriferrioxamine B. The strongest destabilizing effect is due to the shrinkage of the peptidic chains of ligand $\mathbf{L^1}$ compared with ligands $\mathbf{L^2}$ and $\mathbf{L^3}$ (Table 3). The K_1 values related to the monoferric $\mathbf{L^2}$ and $\mathbf{L^3}$ complexes are not very sensitive to the nature of the R_2 substituents. This result suggests that the ferric ion is coordinated by the hydroxamate cavity located in the lower part of the ligands, close to the amine anchor.

Clearly, bulkier R_2 substituents increase the stability of the diferric complex, as revealed by comparison of the K_2 values for $\mathbf{L^3}$ and $\mathbf{L^2}$, which have identical spacers between the anchor and the first hydroxamate binding site. The shortening of the latter spacers in $\mathbf{L^1}$ relative to $\mathbf{L^2}$ and $\mathbf{L^3}$ also induces an increase in the K_2 values of the dinuclear $\mathbf{L^1}$ complex.

The K_2/K_1 ratio enables us to quantify the interactions between the metal centers in the trihydroxamate helicoidal structures (Table 3). These interactions are minimal for ligand $\mathbf{L^3}$, which possesses long spacers between the anchor and the first hydroxamate groups, and bulky R_2 substituents: the two trihydroxamate iron(III) binding cavities behave statistically. Negative cooperativity is observed between the two centers of ligand $\mathbf{L^2}$, which lacks R_2 substituents. The transition from negative cooperativity in $\mathbf{L^2}$ to statistical behavior in $\mathbf{L^3}$ mostly derives from a higher K_2 value in $\mathbf{L^3}$ than in $\mathbf{L^2}$ (Table 3). This is ascribed to the presence of the aspartic linker in $\mathbf{L^3}$ instead of the β-alanyl linker in $\mathbf{L^2}$. The aspartyl linker presumably enhances K_2 by forming a belt of H-bonds with the ligand's backbone amides. This explanation is supported by the enhanced chiral preference of this ligand's ferric complexes, as reported in the Experimental Section. Positive cooperativity

Table 3. Interactions in the Dinuclear Complexes[a,b]

ligand	$\log K_1 \pm 3\sigma$	$\log K_2 \pm 3\sigma$	$\log K_3 \pm 3\sigma$	$K_2/K_1 \pm 3\sigma$
$\mathbf{L^1}$	5.82 ± 0.05	6.32 ± 0.08	4.7 ± 0.1	3.2 ± 0.4
$\mathbf{L^2}$	6.60 ± 0.03	5.50 ± 0.08	5.1 ± 0.1	0.08 ± 0.01
$\mathbf{L^3}$	6.75 ± 0.04	6.05 ± 0.09	4.8 ± 0.1	0.20 ± 0.02

[a] Solvent methanol; p[H] = 6.5 ± 0.1; I = 0,05 M; T = 25.0 ± 0.1 °C;

$$L + Fe(III) \overset{K_1}{\rightleftharpoons} LFe(III); \quad LFe(III) + Fe(III) \overset{K_2}{\rightleftharpoons} LFe(III)_2;$$

$$LFe(III)_2 + Fe(III) \overset{K_3}{\rightleftharpoons} LFe(III)_3$$

K_2, K_1, and K_3 correspond to average values of the data fitted with the Letagrop software.[62,63] With an experimental error of $\pm 3\sigma$ and a number of experimental points larger than 300, the confidence interval is equal to 99.7%. [b] Cooperative effects[5] are defined positive when $K_2/K_1 > 0.25$, negative when $K_2/K_1 < 0.25$, and statistical when $K_2/K_1 = 0.25$.

in favor of the dinuclear complex is achieved with ligand $\mathbf{L^1}$, which possesses short spacers between the anchor and the first binding site, and shows a smaller stability constant for its monoferric complex. Hence, the cooperative behavior of the three diferric helicoidal complexes can be drastically tuned by minor changes in the chemical structure of tripodal ligands.

The stability of ferric complexes with unsubstituted (R_N = H) dihydroxamate ligands having from four to eight methylene groups in the alkane bridge was previously studied.[68] More recently substituted dihydroxamic acids (R_N = CH_3) with spacers possessing from two to eight methylene groups were considered.[54] In the series of the unsubstituted compounds, a shortening of the spacers results in a decrease of the overall complex stability, and elongation of the spacers to seven or more methylene groups results in a significant increase of complex stability. In the substituted compounds, which are better models for our ligands, the formation of monomeric dihydroxamate ferric complexes occurs with spacers of at least six methylene groups. The triple-stranded ligands $\mathbf{L^1}$, $\mathbf{L^2}$, and $\mathbf{L^3}$ possessing spacers of six atoms between the two hydroxamate moieties do also form triferric dihydroxamate complexes, as expected from the latter studies. The close K_3 values determined for the triferric complexes of $\mathbf{L^1}$, $\mathbf{L^2}$, and $\mathbf{L^3}$ (Table 3) are thus in agreement with the trends reported in the previous studies,[68,54] which demonstrated the predominant influence of the length of the spacers on the stability of the complexes. The small variations in the K_3 values are attributed to changes in the R_1 and R_2 substituents.

The distribution curves (Figure 6) of the three ferric complexes formed with ligands $\mathbf{L^1}$, $\mathbf{L^2}$, and $\mathbf{L^3}$ at a given concentration of free ligand (10^{-4} M) and increasing concentrations of iron(III) have been calculated using the Haltafall program,[69] and the respective stability constants are given in Table 3. The formation of the triferric complex starts for the three ligands considered at a $[Fe(III)]_{tot}/[ligand]_{tot}$ ratio of about 1.2. When iron(III) is in large excess (i.e., $[Fe(III)]_{tot}/[ligand]_{tot} > 3$), this species is predominant. Figure 6 clearly shows that the formation of the monoferric complex is strongly favored by the chemical structure of ligand $\mathbf{L^2}$ and the formation of the dinuclear helicate by that of ligand $\mathbf{L^1}$, while competition with an open triferric species occurs in all three compounds.

It is important to emphasize that the assignment of the species deduced from ESMS yielded the best fit with the spectrophotometric data.[46−55] Moreover, the major species detected by ESMS matched the major species observed by absorption spectrophotometry at given ligand:iron stoichiometries, such that all quantitative trends were found to be identical (Table 4). Accurate quantitative data were obtained from the spectrophotometric titrations.

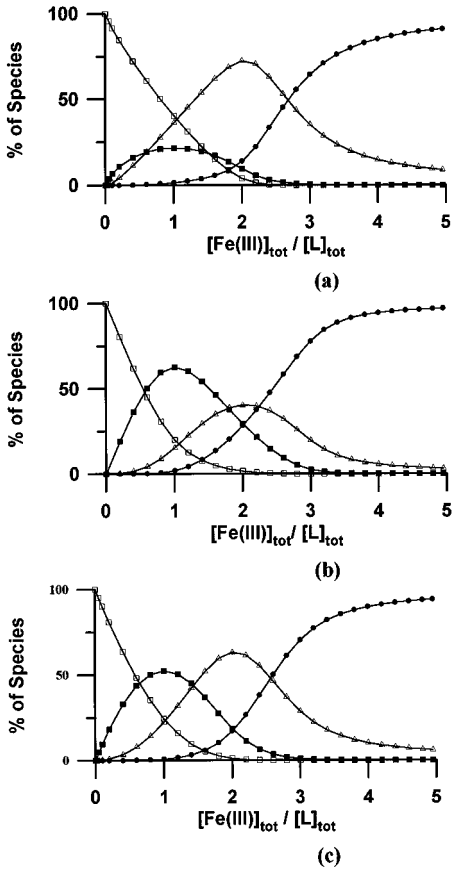

Figure 6. Distribution curves (□, **L**; ■, **L**Fe; △, **L**Fe_2; ●, **L**Fe_3) of the (a) $\mathbf{L^1}$, (b) $\mathbf{L^2}$, and (c) $\mathbf{L^3}$ ferric complexes: solvent methanol; p[H] = 6.5 ± 0.1; I = 0.05; T = 25.0 ± 0.1 °C; $[\mathbf{L}]_{tot} = 10^{-4}$ M. The stability constants are given in Table 3.

Table 4. ESMS Data: Distribution of the Ferric $\mathbf{L^1}$ Complexes in Methanol[a]

$[Fe(III)]_{tot}/[\mathbf{L^1}]tot$	% $\mathbf{L^1}$	% $\mathbf{L^1}$Fe	% $\mathbf{L^1}Fe_2$	% $\mathbf{L^1}Fe_3$
0.5	17	56	27	0
0.7	11	58	31	0
1.2	12	24	63	0
1.5	0	0	100	0
1.7	0	5	95	0
2.0	0	0	88	12
2.5	0	0	57	43
5.0	0	0	0	100

[a] The proportion of the nth species was directly deduced from the relative intensity I_n (n = 1, 2, 3, 4) of its ESMS peak by the formula $I_n/\sum_{n=1-4} I_n$.

The maximal absorbtivities of the various $\mathbf{L^1}$, $\mathbf{L^2}$, and $\mathbf{L^3}$ ferric complexes are presented in Table 5. The broad charge-transfer band is centered at 435 nm for all the mono- and diferric complexes. The extinction coefficients of the monoferric complexes (4300 ± 500 M^{-1} cm^{-1}) show classical values for ferric trihydroxamate complexes.[70−72] The extinction coefficients determined at the absorbance maxima are higher than that of ferrioxamine B (Table 5) or those of various trihydrox-

(68) Evers, A.; Hancock, R. D.; Martell, A. E.; Motekaitis, R. J. *Inorg. Chem.* **1989**, *28*, 2189−2195.
(69) Ingri, N.; Kakolowicz, W.; Sillen, L. G.; Warnqvist, B. *Talanta* **1967**, *14*, 1261−1286.
(70) Konetschny-Rapp, S; Jung, G.; Raymond, K. N.; Meiwes, J.; Zähner, H. *J. Am. Chem. Soc.* **1992**, *114*, 2224−2230.
(71) Ng, C. Y.; Rodgers, S. J.; Raymond, K. N. *Inorg. Chem.* **1989**, *28*, 2062−2066.
(72) Wong, G. B.; Kappel, M. J.; Raymond, K. N.; Matzanke, B.; Winkelmann, G. *J. Am. Chem. Soc.* **1983**, *105*, 810−815.

Table 5. $\mathbf{L^1}$, $\mathbf{L^2}$ and $\mathbf{L^3}$ Ferric Complexes: Maximal Absorbtivities[a]

complexes	λ_{max} (nm)	ϵ_{max} (M^{-1} cm^{-1})	complexes	λ_{max} (nm)	ϵ_{max} (M^{-1} cm^{-1})
$\mathbf{L^1}$Fe	435 ± 2	4300 ± 500	$\mathbf{L^1}Fe_2$	435 ± 2	6500 ± 200
$\mathbf{L^2}$Fe	430 ± 2	4100 ± 200	$\mathbf{L^2}Fe_2$	445 ± 2	7300 ± 300
$\mathbf{L^3}$Fe	425 ± 2	4300 ± 300	$\mathbf{L^3}Fe_2$	435 ± 2	7200 ± 200
ferrioxamine B	429 ± 2	2800 ± 200	$\mathbf{L^1}Fe_3$	460 ± 2	6000 ± 500
			$\mathbf{L^2}Fe_3$	450 ± 2	3700 ± 400
			$\mathbf{L^3}Fe_3$	445 ± 2	5200 ± 200

[a] Solvent methanol; p[H] = 6.5 ± 0.1; I = 0.05 M; T = 25.0 ± 0.1 °C.

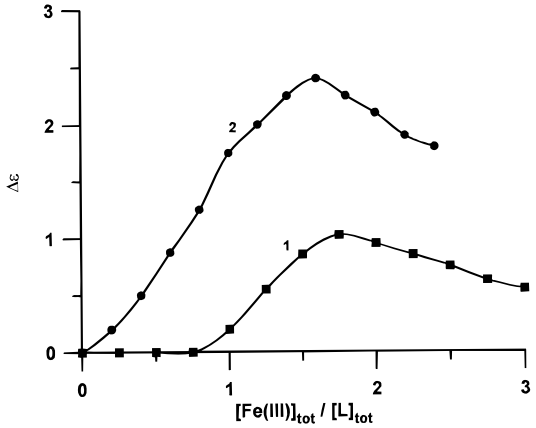

Figure 7. CD titration of ligands $\mathbf{L^2}$ and $\mathbf{L^3}$ with Fe(III): solvent methanol; p[H] = 6.3 ± 0.1 with dichloroacetic buffer, 5 × 10^{-2} M; [**L**] = 10^{-4} M; T = 25.0 ± 0.1 °C; spectrum 1, $\mathbf{L^2}$; spectrum 2, $\mathbf{L^3}$. The data given are absolute dichroic values measured at 375 nm for $\mathbf{L^2}$ and at 460 nm for $\mathbf{L^3}$. The longer wavelength values were chosen for $\mathbf{L^3}$, because they show minimal overlap with other chromophores. The shorter wavelength values were chosen for $\mathbf{L^2}$, since its complexes' small ellipticities at longer wavelength were conceived less reliable. $\Delta\epsilon = \epsilon(L) - \epsilon(R)$, the difference of the absorption coefficient between left and right circularly polarized light (M^{-1} cm^{-1}).

amate species (425 nm < λ_{max} < 450 nm; 2400 M^{-1} cm^{-1} < ϵ_{max} < 3800 M^{-1} cm^{-1}).[70−72] This observation probably derives from increased strain in the tripodal cavity close to the anchor, when compared with the strain-free cavity formed by ferrioxamine B or by bidentate hydroxamic acids. The extinction coefficients of the diferric complexes are slightly smaller than twice the value calculated for the monoferric species. This is probably due to a slightly different coordination geometry of both cations in the dinuclear helicates and to different electronic properties of the hydroxamates' substituents. A shift toward higher wavelengths (460 nm) is observed for the triferric complexes. This behavior is characteristic for dihydroxamate ferric complexes (470 nm < λ_{max} < 480 nm; 1700 M^{-1} cm^{-1} < ϵ_{max} < 2100 M^{-1} cm^{-1}).[23,73] The highest extinction coefficient corresponding to the 3-fold classical dihydroxamate value is observed for the triferric complex formed with the shortest, nonsubstituted ligand $\mathbf{L^1}$ (Table 5). The extinction coefficients of $\mathbf{L^2}Fe_3$ and $\mathbf{L^3}Fe_3$ are very sensitive to the R_2 substituent (Table 5): absence of the substituent drastically decreases the ϵ_{max} value. One can well rationalize that folding of the arms around three iron(III) cations is very sensitive to the chain length and to the steric hindrance of lateral substituents.

CD titrations of the chiral ligands $\mathbf{L^2}$ and $\mathbf{L^3}$ with iron(III) (Figure 7) qualitatively support the conclusions drawn from the analysis of the spectrophotometric titration experiments. The molar ellipticity is small for $\mathbf{L^2}$ up to 0.75 equiv of iron(III), reaches a maximum around 1.75 equiv, and falls off thereafter. These data are in compliance with the predominant formation of a mononuclear complex at low iron(III) concentrations which lacks chiral preference. At higher concentrations the diferric complex is formed with some degree of helicity, and at still higher concentrations the triferric complex which exhibits low chiral preference becomes predominant. For $\mathbf{L^3}$, the molar ellipticity increases almost linearly up to the addition of 1.5 equiv of iron(III), and falls off thereafter. These observations are compatible with the formation of both mononuclear and dinuclear complexes of helical nature[74] up to 1.2 equiv of iron(III). At higher concentrations, triferric complexes of little chiral preference are formed.

Conclusion

The synthesis of three tripodal, polytopic binders is described. Their iron(III) coordination properties have been investigated by applying a combination of electron spray mass spectrometry and UV−vis and CD absorption spectrophotometry. Quite remarkably, subtle structural variations proved to tune these compounds' coordination properties and to provide representatives of opposite cooperative behavior. The observation of positive cooperativity for the achiral ligand $\mathbf{L^1}$ is of relevance for the synthesis of extended helicates incorporating more than two metal ions. Identification of the necessary structural elements for achieving positive cooperativity has direct bearings for the synthesis of heteronuclear metal complexes and structurally related molecular redox switches.[39] These possibilities are under current consideration, as are further structural variations to amplify positive cooperative behavior.

Experimental Section

Synthesis. ^{1}H NMR spectra were measured on a Bruker WH 270 or on a Bruker AMX 400 spectrometer, at concentrations of (1−2) × 10^{-2} M. Chemical shifts are reported in parts per million on the δ scale relative to tetramethylsilane (TMS) as internal standard. Infrared spectra were recorded on a Nicolet 510 FT-IR spectrometer at concentrations of (1−2) × 10^{-2} M. Absorption frequencies are given in inverse centimeters. Circular dichroism (CD) spectra were measured on a Jasco J-500C spectropolarimeter, and the dichroic values $\Delta\epsilon$ are given in M^{-1} cm^{-1} units. Purifications were performed by column chromatography, using silica gel 60 (70−230 mesh ASTM) or flash chromatography using silica gel 60 (230−400 mesh ASTM). TLC examinations were performed using Merck TLC precoated aluminum sheets. Solvents and commercially available reagents were of analytical grade. Protected amino acids were purchased from Sigma. The following abbreviations have been used: Ar, aryl; Bn, benzyl; Boc, *tert*-butyloxycarbonyl; DCC, *N*,*N*′-dicyclohexylcarbodiimide; DICD, *N*,*N*′-diisopropylcarbodiimide; DMAP, 4-(dimethylamino)pyridine; Et, ethyl; Ph, phenyl; TFA, trifluoroacetic acid.

General Coupling Procedure. To a cold solution of protected amino acid (1.0 equiv) and 1-hydroxybenzotriazole (0.1 equiv) (Fluka) in acetonitrile dried over basic alumina were added amine (1.1 equiv) and *N*,*N*′-diisopropylcarbodiimide (1.1 equiv) (Fluka). The reaction mixture was kept at 0−4 °C for 1−3 h and then at room temperature overnight. The solution was concentrated and the product purified using column chromatography.

General Procedure for Hydrolysis of Ethyl or Methyl Esters. Ethyl or methyl ester (1 mmol) was dissolved in methanol (10 mL) and treated with 1 M aqueous sodium hydroxide solution (1.25 mL) at room temperature. The reaction mixture was monitored by TLC every hour, and additional 1.25 mL portions of aqueous sodium hydroxide solution were added until all starting material was consumed. The mixture was cooled in an ice bath and acidified with $KHSO_4$ to pH 2. Methanol was evaporated, and the residue was extracted with ethyl acetate. The organic fraction was washed with water, dried over $MgSO_4$, and concentrated to afford the acid.

(73) Harris, W. R.; Carrano, C. J.; Raymond, K. N. *J. Am. Chem. Soc.* **1979**, *101*, 2722−2727.

(74) van der Helm, D.; Baker, J. R.; Eng-Wilmot, D. L.; Hossain, M. B.; Loghry, R. A. *J. Am. Chem. Soc.* **1980**, *102*, 4224−4231.

Procedure for Solid State Oligomerization. The synthesis was performed using chloromethylated polystyrene−2% divinylbenzene resin (Merck). The first unit was attached to the resin by mixing the acid (3.4 mmol) in absolute ethanol (14 mL) with triethylamine (0.43 mL, 3 mmol) and polymeric resin (2.3 g) for 72 h at 80 °C. Subsequent coupling steps on the polymeric support were carried out with freshly prepared 1-hydroxybenzotriazole active esters of the monomer acids in acetonitrile/methylene chloride (85/15 v/v) at room temperature overnight. The active esters were prepared 2−3 h prior to each coupling step by mixing monomer acid (2.0 mmol), 1-hydroxybenzotriazole (2.0 mmol), and *N*,*N*′-diisopropylcarbodiimide (2.2 mmol) in acetonitrile at 0 °C.

(I) Ligand Synthesis. Intermittent Monomer 2. Condensation of 6.4 g (33.8 mmol) of *N*-Boc-*β*-alanine with 3-[*N*-(benzyloxy)amino]-propionic acid ethyl ester[75,76] (**1**) (8.29 g, 37.2 mmol) according to the general coupling procedure provided 8.6 g (21.8 mmol, 64% yield) of product **2**. ^{1}H NMR ($CDCl_3$): δ 7.35 (m, 5H, Ph), 5.19 (br, 1H, N*H*), 4.78 (s, 2H, PhCH_2O), 4.06 (q, J = 7.1Hz, 2H, OCH_2CH$_3$), 3.95 (m, 2H, CH_2NO), 3.36 (m, 2H, NCH_2), 2.57 (m, 4H, CH_2CO), 1.19 (t, J = 7.1 Hz, 3H, CH_3). FT-IR ($CDCl_3$, cm^{-1}): ν 1715 (C═O ester), 1672 (C═O Boc and hydroxamate).

Terminal Monomer 3. 3-[*N*-(Benzyloxy)amino]propionic acid ethyl ester[75,76] (**1**) (6.84 g, 30.6 mmol) was dissolved in 300 mL of dry toluene and treated under ice, cooling first with 3.8 mL (30.4 mmol) of triethylamine and then dropwise with 2.8 mL (26 mmol) of anisoyl chloride dissolved in 50 mL of toluene. Then, the mixture was stirred under cooling for 1 h and at room temperature for 1 h. The reaction mixture was then washed with 1 M aqueous HCl, water, 1 M $NaHCO_3$, and water and dried over $MgSO_4$. Concentration of the organic phase and chromatography using hexane/ethyl acetate (7/3 v/v) as eluent provided 7.45 g (22 mmol, 74.4% yield) of the ethyl ester of monomer **3**. ^{1}H NMR ($CDCl_3$): δ 7.68, 6.85 (ABq, J = 8.7 Hz, 4H, anisoyl), 7.30−7.26 (m, 5H, Ph), 4.66 (s, 2H, PhCH_2O), 4.06 (q + t, 4H, OCH_2-CH$_3$ and CH_2NO), 3.84 (s, 3H, OCH_3), 2.69 (t, J = 6.6 Hz, 2H, CH_2-CO), 1.20 (t, J = 6.6 Hz, 3H, CH_3). FT-IR ($CDCl_3$, cm^{-1}): ν 1729 (C═O ester), 1631 (C═O hydroxamate). Hydrolysis of the ester according to the general procedure afforded the monomer acid **3** in 49% yield. ^{1}H NMR ($CDCl_3$): δ 7.7, 6.88 (ABq, J = 8.7 Hz, 4H, anisoyl), 7.29−7.15 (m, 5H, Ph), 4.67 (s, 2H, PhCH_2O), 4.06 (t, J = 6.8 Hz, 2H, CH_2NO), 3.85 (s, 3H, OCH_3), 2.74 (t, J = 6.8 Hz, 2H, CH_2CO). FT-IR ($CDCl_3$, cm^{-1}): ν 1714 (C═O acid), 1629 (C═O hydroxamate).

Protected Ion Binding Chain 6. Terminal monomer acid **3** was activated by treating 2.2 g (7.35 mmol) of acid in 50 mL of acetonitrile with 1.95 g (7.3 mmol) of pentachlorophenol, 150 mg of DMAP, and 1.2 mL (7.6 mmol) of DICD under cooling. After being stirred for two days, the crude mixture was concentrated and chromatographed first on neutral alumina (activity V) using chloroform as eluent and then on silica gel (chloroform/hexane, 9/1 v/v) to provide 2.68 g (4.9 mmol, 64.9% yield) of activated ester **5**. Mp: 103−106 °C. ^{1}H NMR ($CDCl_3$): δ 7.75, 6.92 (ABq, J = 8.7 Hz, 4H, anisoyl), 7.30−7.20 (m, 5H, Ph), 4.70 (s, 2H, PhCH_2O), 4.19 (t, J = 6.9 Hz, 2H, CH_2NO), 3.87 (s, 3H, OCH_3), 3.12 (t, J = 6.9 Hz, 2H, CH_2CO). FT-IR ($CDCl_3$, cm^{-1}): ν 1780 (C═O active ester), 1633 (C═O hydroxamate). Intermittent monomer **2** was deprotected by treating 2.5 g (6.34 mmol) of compound with 4 mL of TFA in 8 mL of methylene chloride for 30 min at room temperature to provide **4**. A 2.0 g sample of the corresponding ammonium salt was dissolved in 1 mL of DMF, neutralized with triethylamine, and then treated with 3.2 g (5.8 mmol) of activated monomer **5** dissolved in 20 mL of methylene chloride in the presence of 100 mg of imidazole. The reaction mixture was stirred overnight at room temperature, concentrated, and chromatographed on silica gel using chloroform as eluent to provide the ethyl ester **6**. ^{1}H NMR ($CDCl_3$): δ 7.75, 6.86 (ABq, J = 8.7 Hz, 4H, anisoyl), 7.36−7.27 (m, 10H, Ph), 6.5 (br t, 1H, N*H*), 4.74 (s, 2H, PhCH_2O), 4.67 (s, 2H, PhCH_2O), 4.07 (m, 4H, CH_2NO and OCH_2), 3.95 (m, 2H, CH_2-NO), 3.84 (s, 3H, OCH_3), 3.45 (m, 2H, CH_2NH), 2.55 (m, 6H, CH_2-CO), 1.19 (t, J = 4.8 Hz, 3H, CH_3). FT-IR ($CDCl_3$, cm^{-1}): ν 1728 (C═O ester), 1670 (C═O amide and hydroxamate).

Protected Ion Binding Chain 7. Hydrolysis of ester **6** according to the general hydrolysis procedure provided the free acid. ^{1}H NMR ($CDCl_3$): δ 7.60, 6.80 (ABq, J = 8.7 Hz, 4H, anisoyl), 7.30−7.12, (m, 10H, Ph), 6.65 (br t, 1H, N*H*), 4.76 (s, 2H, PhCH_2O), 4.63 (s, 2H, PhCH_2O), 3.93 (m, 4H, CH_2NO), 3.84 (s, 3H, OCH_3), 3.49 (m, 2H, CH_2NH), 2.58−2.52 (m, 6H, CH_2CO). FT-IR ($CDCl_3$, cm^{-1}): ν 1728 (C═O acid), 1670 (C═O amide and hydroxamate). Then, 2.0 g (3.6 mmol) of acid dissolved in 20 mL of acetonitrile was treated with 1.25 g (4.7 mmol) of pentachlorophenol, 450 mg of DMAP, and 0.8 mL (5.1 mmol) of DICD overnight. The resulting mixture was concentrated and chromatographed on silica gel (elution with hexane/chloroform, chloroform, and chloroform/ethyl acetate mixtures) to provide 1.69 g (1.95 mmol, 54% yield) of the active ester **7**. ^{1}H NMR ($CDCl_3$): δ 7.68, 6.87 (ABq, J = 8.7 Hz, 4H, anisoyl), 7.34, 7.28, 7.15 (m, 10H, Ph), 6.50 (br t, 1H, N*H*), 4.82 (s, 2H, PhCH_2O), 4.65 (s, 2H, PhCH_2O), 4.01 (m, 4H, CH_2NO), 3.84 (s, 3H, OCH_3), 3.51 (m, 2H, CH_2NH), 2.96 (t, J = 6.9 Hz, 2H, CH_2COOC$_6$Cl$_5$), 2.57 (m, 4H, CH_2CO). FT-IR ($CDCl_3$, cm^{-1}): ν 1780 (C═O active ester), 1663 (C═O amide and hydroxamate).

Ligand L^1. A 225 mg (0.27 mmol) sample of active ester **7** was dissolved in 10 mL of methylene chloride and stirred under argon with 0.010 mL (0.07 mmol) of tris(2-aminoethyl)amine (TREN, **8**) and 20 mg of *N*-hydroxysuccinimide overnight. Then the mixture was concentrated and chromatographed on silica gel with chloroform/methanol as eluent to provide 84 mg (0.045 mmol, 64.2% yield) of benzyl-protected ligand **L^1** (R = Bn). ^{1}H NMR ($CDCl_3$): δ 7.7, 6.90 (ABq, J = 8.7 Hz, 12H, anisoyl), 7.40−7.15 (m, 30H, Ph), 4.80 (m, 6H, PhCH_2O), 4.75 (s, 6H, PhCH_2O), 4.10 (m, 6H, CH_2NO), 3.97 (m, 6H, CH_2NO), 3.80 (s, 9H, OCH_3), 3.50 (m, 6H, CH$_2$CH_2NH), 3.10 (m, 6H, CH$_2$CH_2NH), 2.6 (m, 6H, NCH_2CH$_2$NH), 2.50−2.45 (m, 12H, CH_2CO), 2.45 (m, 6H, CH_2CO). FT-IR ($CDCl_3$, cm^{-1}): ν 1653 (C═O amide and hydroxamate). A 200 mg (0.01 mmol) sample of protected ligand **L^1** (R = Bn) was dissolved in 50 mL of ethanol and hydrogenated under atmospheric pressure in the presence of 75 mg of Pd/C (10%) for 6 h. Filtration and concentration of the filtrate provided 104 mg of **L^1** (0.008 mmol, 80% yield). Mp: 140−145 °C. ^{1}H NMR ($CDCl_3$/CD_3OD): δ 7.7, 6.90 (ABq, J = 8.7 Hz, 12H, anisoyl), 3.96 (m, 6H, CH_2NO), 3.86 (m, 6H, CH_2NO), 3.80 (s, 9H, OCH_3), 3.43 (m, 6H, CH$_2$CH_2NH), 3.29 (m, 6H, CH$_2$CH_2NH), 2.6 (m, 6H, NCH_2CH$_2$-NH), 2.57−2.51 (m, 18H, CH_2CO). The assignment of the ligand's ^{1}H-NMR signals was confirmed by correlation spectroscopy (COSY), which showed cross-peaks for each of the compound's ethylene bridges and for the two aromatic signals. FT-IR (KBr, cm^{-1}): ν 1644 (C═O amide and hydroxamate).

Ligand L^2. Protected ligand **L^2** (R = Bn) was prepared by condensation of active ester **7** with trisamine **9**[65] as described for the preparation of protected ligand **L^1**. ^{1}H NMR (CD_3OD, 10 mM): δ 7.56, 6.88 (ABq, J = 8.7 Hz, 12H, anisoyl), 7.35−7.13 (m, 30H, Ph), 4.76 (m, 6H, PhCH_2O), 4.66 (m, 6H, PhCH_2O), 4.39 (m, 3H, C*H*-*i*-Bu), 4.03 (m, 6H, CH_2NO), 3.91 (m, 3H, CH_2NO), 3.79 (s + m, 12H, OCH_3 + CH_2NO), 3.37 (m, 12H, CH$_2$CH_2NH), 2.55 (m, 24H, CH_2CO and NCH_2CH$_2$NH), 1.60 (br, 9H, CH_2{*i*-Bu} + C*H*{*i*-Bu}), 0.87−0.82 (m, 18H, CH_3{*i*-Bu}). FT-IR ($CDCl_3$ 1.6 mM, cm^{-1}): ν 3300 (NH), 1656, 1650, 1644 (C═O amide and hydroxamate). Hydrogenation of protected ligand **L^2** (R = Bn) as described for protected ligand **L^1** provided the free ligand **L^2**. Mp: 105−110 °C. ^{1}H NMR (CD_3OD, 8 mM): δ 7.66, 6.93 (ABq, J = 8.7 Hz, 12H, anisoyl), 4.36 (m, 3H, C*H*-*i*-Bu), 3.97 (m, 6H, CH_2NO), 3.86 (m, 6H, CH_2NO), 3.82 (s, 9H, OCH_3), 3.65 (m, 3H, CH$_2$CH_2NH), 3.45 (m, 9H, CH$_2$CH_2NH), 2.67 (m, 6H, NCH_2CH$_2$NH), 2.60 (m, 18H, CH_2CO), 1.65 (m, 9H, CH_2{*i*-Bu} + C*H*{*i*-Bu}), 0.93−0.88 (m, 18H, CH_3{*i*-Bu}). FT-IR (KBr, cm^{-1}): ν 3284 (NH), 1657, 1650, 1643 (C═O amide and hydroxamate).

***N*-Boc-L-Aspartic Acid α-Diethyl Amide *β*-Benzyl Ester.** Condensation of *N*-Boc-L-aspartic acid *β*-benzyl ester and diethylamine according to the general coupling procedure, followed by column chromatography using hexane/ethylacetate (1/1) as eluent, provided the product in 41% yield. ^{1}H NMR ($CDCl_3$): δ 7.34 (s, 5H, Ph), 5.33 (d, J = 9.4 Hz, 1H, N*H*), 5.11 (m, 2H, CH_2Ph), 4.95 (m, 1H, C*H*), 3.44 (m, 2H, NCH_2CH$_3$(trans)), 3.29 (m, 2H, NCH_2CH$_3$(cis)), 2.85 (dd, J_{gem} = 15.8 Hz, J_{vic} = 7.0 Hz, 1H, CHCH_2), 2.65 (dd, J_{gem} = 15.7 Hz, J_{vic}

(75) Yakirevitch, P.; Rochel, N.; Albrecht-Gary, A. M.; Libman, J.; Shanzer, *A. Inorg. Chem.* **1993**, *32*, 1779−1787.

(76) Yakirevitch, P. Ph.D. Thesis, The Feinberg Graduate School of the Weizmann Institute of Science, Rehovot, Israël, 1992.

= 5.8 Hz, 1H, CHCH_2), 1.42 (s, 9H, *t*-Bu), 1.23 (t, J = 7.1 Hz, 3H, NCH$_2$CH_3(cis)), 1.09 (t, J = 7.1 Hz, 3H, NCH$_2$CH_3(trans)). FT-IR (neat, cm^{-1}): ν 3297 (NH), 1738 (C═O ester), 1710 (C═O Boc), 1641 (C═O amide).

***N*-Boc-L-aspartic Acid α-Diethyl Amide.** To a solution of *N*-Boc-L-aspartic acid α-diethyl amide β-benzyl ester (1.5 g, 4.017 mmol) in absolute ethanol (100 mL) was added 300 mg Pd/C (10%, and the reaction mixture was hydrogenated for 2 h at room temperature and atmospheric pressure. The catalyst was filtered off, and the solvent was evaporated, affording the free acid in 92% yield. ^{1}H NMR (CDCl$_3$): δ 5.6 (br d, 1H, N*H*), 5.0 (m, 1H, C*H*), 3.71 (q, J = 7.0 Hz, 2H, NCH_2CH$_3$(trans)), 3.42 (m, 2H, NCH_2CH$_3$(cis)), 2.71 (m, 2H, CHCH_2), 1.43 (s, 9H, *t*-Bu), 1.31−1.01 (m, 6H, NCH$_2$CH_3). FT-IR (CDCl$_3$, cm^{-1}): ν 3299 (br, NH, OH), 1713 (C═O acid, Boc), 1634 (C═O amide).

Intermittent Monomer Acid 10. Boc-L-aspartic acid α-diethyl amide and 3-[*N*-(benzyloxy)amino]propionic acid ethyl ester (**1**)[75,76] were reacted according to the general coupling procedure, followed by column chromatography using hexane/ethyl acetate (1/1) as eluent, to afford the ethyl ester of **10** in 85% yield. ^{1}H NMR (CDCl$_3$): δ 7.34 (s, 5H, Ph), 5.24 (m, 1H, C*H*), 4.86 (s, 2H, PhCH_2O), 4.04 (m, 4H, CH_2NO and OCH_2CH$_3$), 3.42 (m, 4H, NCH_2CH$_3$), 2.78 (m, 2H, CHCH_2), 2.59 (br t, 2H, CH_2COO), 1.42 (s, 9H, *t*-Bu), 1.20 (m, 9H, NCH$_2$CH_3 and OCH$_2$CH_3). Hydrolysis according to the general procedure afforded the acid **10** in 97% yield. ^{1}H NMR (CDCl$_3$): δ 7.37 (s, 5H, Ph), 5.60 (br d, 1H, N*H*), 4.88, 4.79 (ABq, J = 10.2 Hz, 3H, CH_2Ph (2H) and C*H* (1H)), 3.95 (br, 2H, CH_2NO), 3.34 (m, 2H, NCH_2CH$_3$(trans)), 3.21 (m, 2H, NCH_2CH$_3$(cis)), 2.78 (dd, J_{gem} = 15.2 Hz, J_{vic} = 6.6 Hz, 1H, CHCH_2), 2.62 (br t + dd, 3H, CHCH_2 (1H) and CH_2COO (2H)), 1.43 (s, 9H, *t*-Bu), 1.16−1.04 (m, 6H, NCH$_2$CH_3). FT-IR (CDCl$_3$, cm^{-1}): ν 3433 (NH), 1710 (C═O acid), 1640 (C═O amide).

Solid-Phase Synthesis of Protected Ion Binding Chain 11. The solid synthesis was carried out according to the general oligomerization procedure, starting with *N*-Boc-L-leucine monohydrate (1.87 g, 7.5 mmol) and 5.0 g of polymeric resin. The aspartyl-derived monomeric unit **10** (2.3 g, 4.9 mmol) was added in the presence of DICD (0.8 mL, 5.2 mmol) in acetonitrile. The synthesis proceeded with the addition of the terminating fragment **3** (1.6 g, 4.9 mmol) in the presence of DICD (0.8 mL, 5.2 mmol) in CH$_3$CN/CH$_2$Cl$_2$ (85/15 v/v) and cleavage of the chain from the resin. The cleavage was performed by suspension of the resin in anhydrous methanol (40 mL/1 g of resin), addition of triethylamine (2.6 mL, 18.7 mmol/1 g of resin), and stirring for 24 h at room temperature. Then the polymer was filtered off and washed with methanol and the solution concentrated to dryness. Flash chromatography (2−5% CH$_3$OH/CH$_2$Cl$_2$) afforded 1.72 g of pure ester **11**. ^{1}H NMR (CDCl$_3$, 25 mM): δ 7.68, 6.87 (ABq, J = 8.8 Hz, 4H, anisoyl), 7.35−7.14 (m, 10H, Ph), 7.06, 6.73 (two br d, 2H, N*H*), 5.20 (m, 1H, C$_a$*H*CON), 4.81, 4.71 (ABq, J = 10.1 Hz, 2H, PhCH_2O), 4.66 (s, 2H, PhCH_2O near anisoyl), 4.55 (m, 1H, C$_a$*H*-*i*-Bu), 4.04 (m, 4H, CH_2NO), 3.84 (s, 3H, PhOCH_3), 3.65 (s, 3H, COOCH_3), 3.4−3.21 (m, 4H, NCH_2CH$_3$), 2.59 (m, 4H, CH_2CO), 2.48 (t, J = 6.3 Hz, 2H, CH_2-CO), 1.55 (br m, 3H, C*H* and CH_2{*i*-Bu}), 1.06 (t, J = 7.0 Hz, 6H, NCH$_2$CH_3), 0.87 (d, J = 6.1, 3H, CH_3{*i*-Bu}), 0.85 (d, J = 6.1 Hz, 3H, CH_3{*i*-Bu}). FT-IR (CDCl$_3$ 10 mM, cm^{-1}): ν 3432, 3334 (NH), 1740 (C═O ester), 1640 (C═O amide, CONOBn).

Hydrolysis of Ion Binding Chain 11. Methyl ester **11** (1.2 g, 1.5 mmol) was dissolved in methanol (7 mL) and treated with 2 M aqueous NaOH (3.0 mL) for 2 h. Usual workup according to the general hydrolysis procedure afforded the acid in 98% yield. ^{1}H NMR (CDCl$_3$): δ 7.66, 6.85 (ABq, J = 8.8 Hz, 4H, anisoyl), 7.33−7.12 (m, 10H, Ph), 5.14 (m, 1H, C*H*CON), 4.79, 4.70 (ABq, J = 10 Hz, 2H, PhCH_2O), 4.66 (s, 2H, PhCH_2O near anisoyl), 4.55 (m, 1H, C*H*-*i*-Bu), 4.1 (m, 4H, CH_2NO), 3.83 (s, 3H, PhOCH_3), 3.34−3.23 (m, 4H, NCH_2-CH$_3$), 2.61−2.50 (m, 6H, CH_2CO), 1.6 (m, 3H, C*H* and CH_2{*i*-Bu}), 1.06 (m, 6H, NCH$_2$CH_3), 0.87 (d, J = 6.1 Hz, 3H, CH_3{*i*-Bu}), 0.85 (d, J = 5.7 Hz, 3H, CH_3{*i*-Bu}). FT-IR (CDCl$_3$, cm^{-1}): ν 3348 (NH), 1725 (w), 1637 (C═O).

Ligand L^3. The above acid (1.22 g, 1.54 mmol) was activated with 1-hydroxybenzotriazole (0.21 g, 1.54 mmol) and DCC (0.35 g, 1.7 mmol) in cold THF (5 mL). The reaction mixture was kept at 0−4 °C for 1 h and then at room temperature for 2 h. The active ester solution was treated with triamine **8** (0.063 mL, 0.42 mmol), and stirred under nitrogen atmosphere at room temperature overnight. *N*,*N*′-Dicyclohexylurea (DCU) was filtered off and washed with cold tetrahydrofuran, and the reaction mixture was evaporated to dryness under *vacuo*. Purification of the products by column chromatography using mixtures of 3−8% methanol/chloroform as eluent afforded the protected ligand **L^3** (R = Bn) as a glassy solid in 48% yield. Mp: 46−48 °C. ^{1}H NMR (CDCl$_3$, 20 mM): δ 7.66, 6.94 (ABq, J = 8.7 Hz, 12H, anisoyl), 7.33−7.11 (m, 30H, Ph), 5.2 (m, 3H, C*H*CON), 4.76 (m, 6H, PhCH_2O), 4.66 (br s, 6H, PhCH_2O near anisoyl), 4.4 (m, 3H, C*H*-*i*-Bu), 4.05−3.9 (m, 12H, CH_2NO), 3.85 (s, 9H, OCH_3), 3.24 (m, 18H, NCH_2CH$_3$ and CH$_2$CH_2NH), 2.9, 2.64, 2.53 (m, 24H, CHCH_2, CH_2CO and NCH_2-CH$_2$NH), 1.60 (br, 6H, CH_2{*i*-Bu}), 1.45 (m, 3H, C*H*{*i*-Bu}), 1.02 (m, 18H, NCH$_2$CH_3), 0.84 (br s, 18H, CH_3{*i*-Bu}). FT-IR (CDCl$_3$, cm^{-1}): ν 3306 (NH, OH), 1639 (C═O). A 0.27 g (1.1 mmol) sample of protected ligand **L^3** was dissolved in methanol (40 mL) and chilled in an ice−water bath. A 100 mg sample of Pd/C (10%) was added, and the suspension was hydrogenated at atmospheric pressure for 2 h. The catalyst was filtered off and washed with methanol. The solvent was evaporated, affording the pure product **L^3** (0.18 g, 88% yield) as a glassy powder. Mp: 133−134 °C. ^{1}H NMR (CD$_3$OD, 20 mM): δ 7.68, 6.94 (ABq, J = 8.8 Hz, 12H, anisoyl), 5.23 (br t, 3H, C*H*CON), 4.31 (br t, 3H, C*H*-*i*-Bu), 3.99 (m, 6H, CH_2NO), 3.82 (s + m, 15H, OCH_3 (9H) and CH_2NO (6H)), 3.44 (m, 12H, NCH_2CH$_3$), 3.33 (m, 6H, CH$_2$CH_2NH), 3.05 (m, 3H, CHCH_2), 2.73, 2.64, 2.56 (m, 21H, CHCH_2 (3H), NCH_2CH$_2$NH (6H) and CH$_2$CH_2CO (12H)), 1.68−1.59 (m, 9H, C*H*{*i*-Bu} and CH_2{*i*-Bu}), 1.12−1.08 (br t, 18H, NCH$_2$CH_3), 0.94 (d, J = 6.2 Hz, 9H, CH_3{*i*-Bu}), 0.90 (d, J = 6.1 Hz, 9H, CH_3-{*i*-Bu}). FT-IR (CDCl$_3$ 5 mM, cm^{-1}): ν 3275 (NH, OH), 1630 (C═O).

(II) Preparation of Ferric Complexes of L^1, L^2, and L^3. The monoferric complexes were prepared by treating methanolic solutions of ligand (3.9×10^{-6} mol in 2 mL of methanol) with 1 equiv of FeCl$_3$ (0.65 mL of 6.0 mM FeCl$_3$ in methanol) and addition of anhydrous sodium acetate until the color changed to orange, pH > 8.0. The reaction mixture was then stirred for 30 min, evaporated, and extracted with methylene chloride (150 mL). The organic solution was washed with water, dried over Na$_2$SO$_4$, and evaporated, affording the ferric complexes as red powders. Yield: 90%. The spectral characteristics of the ferric species using 1 equiv of FeCl$_3$ are as follows. (With **L^1**) FT-IR (CDCl$_3$, cm^{-1}): ν 3318 (NH, OH). (With **L^2**) FT-IR (CDCl$_3$, cm^{-1}): ν 3285 (NH, OH). CD (MeOH): λ_{ext} = 455, 374 nm ($\Delta\epsilon$ = 0.0, +0.6). CD (CDCl$_3$): λ_{ext} = 455, 380 nm ($\Delta\epsilon$ = −0.76, +1.25). (With **L^3**) FT-IR (CDCl$_3$, cm^{-1}): ν 3295 (NH, OH). CD (MeOH): λ_{ext} = 460, 380 nm ($\Delta\epsilon$ = −2.0, +3.7). CD (CDCl$_3$): λ_{ext} = 460, 373 nm ($\Delta\epsilon$ = −2.8, +4.7). Higher loaded ferric complexes were obtained according to the same procedure using 2 equiv of FeCl$_3$ (1.33 mL of 6.0 mM FeCl$_3$/methanol). The spectral characteristics of the corresponding ferric species are as follows. (With **L^1**) FT-IR (CDCl$_3$, cm^{-1}): ν 3305 (NH). (With **L^2**) FT-IR (CDCl$_3$, cm^{-1}): ν 3310 (NH). CD (MeOH)SPCLN λ_{ext} = 470, 390 nm ($\Delta\epsilon$ = −0.6, +1.9). CD (CDCl$_3$): λ_{ext} = 450, 375 nm ($\Delta\epsilon$ = −2.6, +5.12). (With **L^3**) FT-IR (CDCl$_3$, cm^{-1}): ν 3295 (NH). CD (MeOH): λ_{ext} = 461, 370 nm ($\Delta\epsilon$ = −4.0, +6.0). CD (CDCl$_3$): λ_{ext} = 460, 373 nm ($\Delta\epsilon$ = −4.7, +9.1).

Electrospray Mass Spectrometric Measurements. ES mass spectra were obtained on a VG BioQ triple quadrupole with a mass to charge (m/z) range of 4000 (VGBioTech Ltd., Altrincham, U.K.). The ES interface was heated to 70 °C. The sampling cone voltage (V_c) was 60 V. No fragmentation process was observed when the voltage V_c was increased to 150 V. The calibration was performed using multiprotonated ions from horse myoglobin. The resolution was about 600 at m/z = 1000 (with a valley of 10%), and then average masses were measured. Scanning was performed from m/z = 400 to m/z = 1400 in 10 s. The data system was operated as a multichannel analyzer, and several scans were summed to obtain the final spectrum. Nonbuffered solutions containing the **L^1** ligand (2×10^{-5} M) and 0.0, 0.5, 0.7, 1.2, 1.5, 1.7, 2.0, 2.5, and 5.0 equiv of FeCl$_3$ in methanol, respectively, were injected into the mass spectrometer source with a syringe pump (Harvard type 55 1111, Harvard Apparatus Inc., South Natick, MA) at a flow rate of 4 mL/min. The concentration of the ligand **L^2** and the ligand **L^3** was 5×10^{-5} M, and the ligands were tested only with 0.0, 0.5, 1.0, and 2.0 equiv of FeCl$_3$.

Potentiometric and Spectrophotometric Measurements. Solid

samples were quantitatively dissolved in pure methanol (Merck, water-free). Iron(III) solutions were prepared from $FeCl_3 \cdot 6H_2O$ (Merck, p.a.) and back-titrated with $Th(NO_3)_4 \cdot 5H_2O$ (Merck) in the presence of excess EDTA (Merck, Titriplex III, 0.1 M) and xylenol orange (Merck) as indicator. Dichloroacetic buffer[77] (0.05 M) was used to maintain the p[H] value at 6.5 ± 0.1. Tetrabutylammonium hydroxide (Fluka, 25% in methanol) was used for neutralization of a titrated (ca. 0.6 M) dichloroacetic acid (BDH, 99%) solution in methanol. Hydrogen ion concentrations were measured with a combined glass electrode (Ingold, high alkalinity). The Ag/AgCl reference electrode was filled with 0.05 M tetramethylammonium chloride (Fluka, p.a.) in pure methanol. Potential differences were given by a Tacussel Isis 20,000 millivoltmeter. Solutions with known hydrogen ion concentrations in methanol[78−81] were used to verify the linearity of the glass electrode. The solutions were continuously swept with methanol-saturated argon. Two methods were used to obtain spectrophotometric data: titration of the free ligands (10^{-4} M) in 2 cm optical quartz cells (Hellma) by concentrated iron(III) solutions (10^{-3} M) and a batch titration method in 5 mL flasks. For the last method and in order to avoid precipitation of iron(III), the reagents were added in the following order: ligand, iron, and buffer. Although the solutions immediately turned red after addition of iron, the buffer was introduced only 2 h later, which led to an instantaneous color change from cherry-red to orange, indicating the formation of the trihydroxamate complexes. At least 10 solutions were prepared for each titration method, and the $[Fe(III)]_{tot}/[ligand]_{tot}$ ratios ranged between 0.2 and 4.0. The temperature was fixed at 25.0 ± 0.1 °C with a Lauda thermostat. The stability of the various solutions was carefully checked for hours after each addition of iron(III), and UV−vis (300−650 nm) absorption spectra were recorded with a Kontron Uvikon 860 spectrophotometer. In order to check the results obtained from the direct spectrophotometric titration of the free ligand **L¹** by iron(III), a competition experiment between the ferric **L¹** complex and a tetracarboxylic acid, CDTA (*N*,*N*′-1,2-cyclohexanediylbis[*N*-(carboxymethyl)glycine], Merck, Titriplex IV), was also undertaken in buffered methanol (p[H] = 6.5 ± 0.1). The ferric **L¹** complex solution was prepared by mixing 1 equiv of ligand ($[\mathbf{L^1}]_{tot} = 4.5 \times 10^{-5}$ M) with 2 equiv of iron(III) ($[FeCl_3]_{tot} = 9.0 \times 10^{-5}$ M). The dichloroacetic buffer[77] concentration was 0.05 M. Methanolic solutions with $[\mathbf{L^1}]_{tot}/[CDTA]_{tot}$ ratios ranging between 0.2 and 4.0 were spectrophotometrically (300−650 nm) examined using a Kontron Uvikon 941 spectrophotometer and 1 cm Hellma quartz cells. A previous determination of the stability constant of the CDTA ferric complex under identical experimental conditions was necessary to calculate the stability of the **L¹** ferric species. A batch titration in 10 mL flasks of CDTA (8.2×10^{-4} M) by increasing amounts of $FeCl_3$ (8×10^{-5} M ≤ $[Fe(III)]_{tot} \leq 1.40 \times 10^{-3}$ M) was carried out. When equilibrium conditions were reached in all the solutions, UV−vis absorption spectra were recorded using a Kontron Uvikon 860 spectrophotometer in the 250−450 nm range. As a reference for the iron(III) binding properties by a trihydroxamate ligand, the stability constant of the methanesulfonate salt of ferrioxamine B (Desferal, Ciba-Geigy) was determined in methanol at p[H] = 6.3 ± 0.1 fixed with 0.1 M dichloroacetic buffer by a direct spectrophotometric titration ($0 \leq [Fe(III)]_{tot}/[desferriferrioxamine\ B]_{tot} \leq 1.5$). The spectrophotometric data were processed with both the Letagrop-Spefo[62,63] and Specfit[59−61] programs, which adjust the absorbtivities and the stability constants of the species formed at equilibrium. Letagrop-Spefo uses the Newton−Raphson algorithm to solve mass balance equations and a pit-mapping method to minimize the errors and determine the best values of the parameters. Specfit uses factor analysis to reduce the absorbance matrix and to extract the eigenvalues prior to the multiwavelength fit of the reduced data set according to the Marquardt algorithm. The model including all ferric species identified by ESMS led to the best fit of the spectrophotometric data. Apparent stability constants at p[H] = 6.5 ± 0.1 are given in this work. For the sake of simplicity charges and protons are omitted in all the chemical equilibria given here.

Acknowledgment. This work has been supported by the Centre National de la Recherche Scientifique (CNRS). E.L and M.M. thank the CNRS and the Conseil Regional d'Alsace for granting them a Ph.D. fellowship. The collaborative research has been carried out with the help of the French-Israeli Keshet Program. Financial support from the U.S.-Israel Binational Foundation and the Israel Academy of Sciences and Humanities is gratefully acknowledged. A.S. is holder of the Siegfried and Irma Ullman Professorial Chair. This paper is dedicated to the memory of Dr. Jacqueline Libman.

Supporting Information Available: Figures showing the spectrophotometric titration data of CDTA and desferriferrioxamine B by iron(III) (2 pages). See any current masthead page for ordering and Internet access instructions.

JA962472C

(77) Cox, B. G.; Truong, N. V. *J. Chem. Soc., Perkin Trans. 2* **1983**, 515−521.
(78) De Ligny, C. L.; Luykx, P. F. M.; Rehbach, M.; Wieneke, A. A. *Recl. Trav. Chim. Pays-Bas* **1960**, *79*, 699−726.
(79) Gelsema, W. J.; De Ligny, C. L.; Remijnse, A. G.; Blijleven, H. A. *Recl. Trav. Chim. Pays-Bas* **1966**, *85*, 647−660.
(80) Alfenaar, M.; De Ligny, C. L. *Recl. Trav. Chim. Pays-Bas* **1967**, *86*, 1185−1190.
(81) Rondinini, S.; Mussini, P. R.; Mussini, T. *Pure Appl. Chem.* **1987**, *59*, 1549−1560.